A Higher-Accuracy van der Waals Density Functional

Kyuho Lee,[1] Éamonn D. Murray,[1] Lingzhu Kong,[1] Bengt I. Lundqvist,[2,3] and David C. Langreth[1]

[1] *Department of Physics and Astronomy, Rutgers University, Piscataway, New Jersey 08854-8019, USA*
[2] *Department of Applied Physics, Chalmers University of Technology, SE - 41296 Göteborg, Sweden*
[3] *Center for Atomic-scale Materials Design, Department of Physics Technical University of Denmark, DK - 2800 Kongens Lyngby, Denmark*

(Dated: August 17, 2010)

We propose a second version of the van der Waals density functional (vdW-DF2) of Dion et al. [Phys. Rev. Lett. **92**, 246401 (2004)], employing a more accurate semilocal exchange functional and the use of a large-N asymptote gradient correction in determining the vdW kernel. The predicted binding energy, equilibrium separation, and potential-energy curve shape are close to those of accurate quantum chemical calculations on 22 duplexes. We anticipate the enabling of chemically accurate calculations in sparse materials of importance for condensed-matter, surface, chemical, and biological physics.

The van der Waals (vdW) attraction is a quantum-mechanical phenomenon with charge fluctuations in one part of an atomic system that are electrodynamically correlated with charge fluctuations in another. The vdW force at one point thus depends on charge events at another region and is a truly nonlocal correlation effect.

Methods for accurately calculating the vdW interactions are critical to understanding sparse matter, including bulk solids (*e.g.*, layered materials, molecular crystals, and polymers), surface phenomena (*e.g.*, adsorption, water overlayers, and gas separation and storage), and biostructures (*e.g.*, DNA and protein structure).

The exact density functional contains the vdW forces. Unfortunately, we do not have access to it, but approximate versions are abundant. Commonly, the local-density approximation (LDA) and generalized gradient approximation (GGA) are used with quite some success for dense matter, including hard materials and covalently bound molecules. They depend on the density in local and semilocal ways, respectively, however, and give no account of the fully nonlocal vdW interaction.

First-principles approaches for how vdW can be treated in DFT were first proposed for the asymptotic interaction between fragments.[1–3] These ultimately evolved into the van der Waals density functional (vdW-DF) for arbitrary geometries.[4–6] Despite its success for describing dispersion in a breadth of systems better than any other nonempirical method,[7] vdW-DF overestimates equilibrium separations [4,5,7–12] and underestimates hydrogen-bond strength.[13,14]

In this Letter, we propose a second version of the van der Waals density functional (vdW-DF2) employing a more accurate semilocal exchange functional PW86[15,16] and the use of a large-N asymptote gradient correction[17] in determining the vdW kernel. By making a full comparison of potential energy curves (PECs) with accurate quantum chemistry results for 22 molecular duplexes, we show that vdW-DF2 substantially improves (i) equilibrium separations, (ii) hydrogen bond strengths, and (iii) vdW attractions at intermediate separations longer than the equilibrium ones. The improvement in (iii), found via a full PEC comparison, is most critical for important "real-life" applications to sparse matter and biological matter where it is impossible for basic structural units to assume the same separations they would have as binary units in vacuo.

First, we replace revPBE exchange functional[18] with PW86,[15,16] because revPBE is generally too repulsive near the equilibrium separation,[8] and can bind spuriously by exchange alone, although less so than most other local or semilocal functionals. Hence, other exchange functionals [20,21] have been proposed. Recent performance studies of various exchange functionals for weakly interacting atoms[22] and molecules,[19] however, show PW86, with an enhancement factor proportional to $s^{2/5}$ at large reduced density gradient s, to give the most consistent agreement with Hartree-Fock (HF) results, without spurious exchange binding. It also is a good match[23] for the vdW-DF2 correlation kernel, introduced below, although no others were tried.

The key to the vdW-DF method is the inclusion of a long range piece of the correlation energy, $E_c^{\rm nl}[n]$, a fully nonlocal functional of the density n. This piece is evaluated using a "plasmon" pole approximation for the inverse dielectric function, which satisfies known conservation laws, limits, sum rules, and invariances.[4] A single parameter model for the pole position was adopted, with the pole residue set by the law of charge-current continuity (f-sum rule), and the pole position at large wave vector set by the constraint that there be no self-Coulomb interaction. The single parameter is determined locally from electron-gas energy input via gradient corrected LDA.[4]

The nonlocal piece of the correlation energy in both vdW-DF and vdW-DF2 is of the form

$$E_c^{nl}[n] = \int d^3r \int d^3r'\, n(\mathbf{r})\phi(\mathbf{r},\mathbf{r}')n(\mathbf{r}'). \qquad (1)$$

The kernel ϕ is given as a function of $Rf(\mathbf{r})$ and $Rf(\mathbf{r}')$, where R=$|\mathbf{r}-\mathbf{r}'|$ and $f(\mathbf{r})$ is a function of $n(\mathbf{r})$ and its gradient. In fact $f(\mathbf{r})$ is proportional to the exchange-correlation energy density ϵ_{xc} of a gradient corrected LDA at the point $\mathbf{r}$. This arose from the approximately

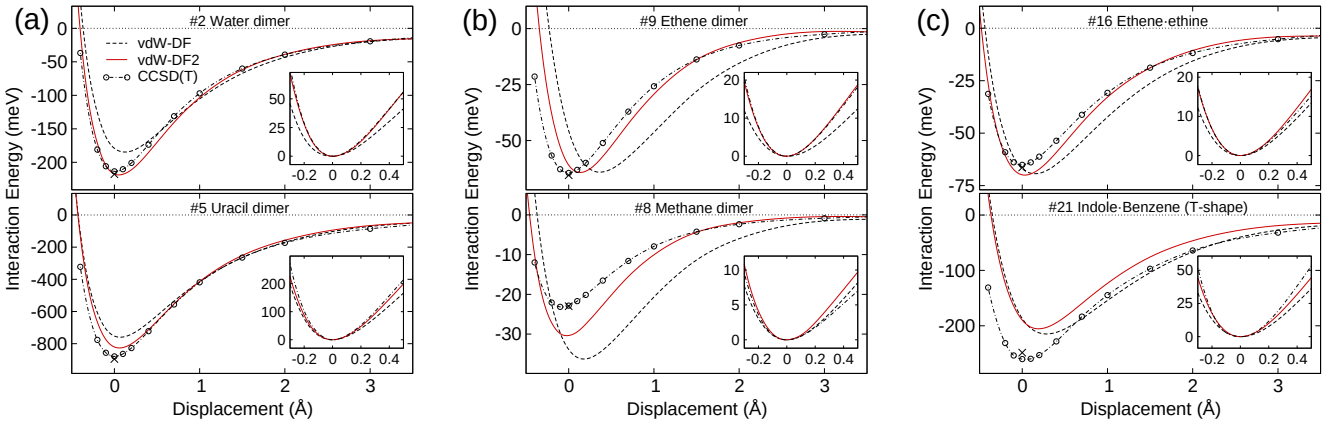

FIG. 1. (Color online) Potential energy curves (PECs) for the best and the worst case of (a) hydrogen-bonded, (b) dispersion-dominated, and (c) mixed duplexes. CCSD(T) QC PECs (dash-dotted lines with circles taken from Ref. 24) and the reference energies (cross marks taken from Ref. 26) at the geometry of Ref. 25 are also shown. The shapes near minima are compared in inset figures where PECs are aligned to have the common minimum point. For all the other S22 duplexes, see Supplemental Material.

implemented requirement that the dielectric function implied by the plasmon pole model should give an exchange-correlation energy semilocally consistent with a gradient corrected electron gas. We call the semilocal functional that fixes $f(\mathbf{r})$ in Eq. (1) the *internal functional*.

The above is easier to understand for two separate molecules, although the arguments apply equally well to a pair of high density regions of a sparse material. The long range vdW attraction implied by Eq. (1) occurs from the contribution where $\mathbf{r}$ is on one molecule and $\mathbf{r}'$ on the other. The definition of $f(\mathbf{r})$ and $f(\mathbf{r}')$ varies continuously and independently at each point according to $\epsilon_{xc}(\mathbf{r})$ and $\epsilon_{xc}(\mathbf{r}')$. The quantity ϵ_{xc} is taken to consist of a gradient corrected LDA. In the first version of vdW-DF,[4] the gradient correction was obtained from a gradient expansion[27] for the slowly varying electron gas.[28,29] More appropriate is a functional that gives accurate energies for *molecules*, however. When $\mathbf{r}$ and $\mathbf{r}'$ are each in a separate molecule-like region, with exponentially decaying tails between them, $f(\mathbf{r})$ and $f(\mathbf{r}')$ can both be large and give key contributions to a vdW attraction. For this case (including perhaps even a molecule near a surface) the large-N asymptote[30,31] and the exchange energy asymptotic series for neutral atoms provide a more accurate approximation. In fact, the exchange parameter[29] β of the B88 exchange functional,[32] successfully used in the vast majority of DFT calculations on molecules, can be derived from first principles using the large-N asymptote,[17] as can the LDA exchange. It seems obvious, then, that vdW-DF results should be improved if the second order expansion of the exchange in gradients is replaced by the second order large-N expansion. Interestingly, PW86R functional, selected as the overall exchange functional for different reasons, also follows the large-N behavior for small reduced gradient s values down to $\sim$0.1, where it reverts to the form of slowly varying electron gas limit.

Thus we use 2.222 times larger exchange gradient coefficient, a value based on agreement between derived[17,30,31] and empirical[32] criteria (a 6% smaller derived value of Ref. 17 only gives a marginal improvement). Assuming that the *screened* exchange term[33] increases in the same proportion as gradient exchange itself, finally we get the appropriate gradient coefficient in the "Z" notation[29] which is multiplied by 2.222. Summarizing: while $Z_{ab} = -0.8491$ in vdW-DF, $Z_{ab} = -1.887$ in vdW-DF2, implying changes in the internal functional.

The performance of our new energy functional is assessed via comparisons with the accurate S22 reference dataset[25,26] and PECs[24] based on quantum chemistry (QC) calculations at the level of CCSD(T) with extrapolation to the complete basis set limit. These twenty-two small molecular duplexes for the non-covalent interactions typical in biological molecules include hydrogen-bonded, dispersion-dominated, and mixed duplexes. Recent evaluation[13] of the performance of the vdW-DF for S22 shows it to be quite good, except for H-bonded duplexes, where vdW-DF underestimates the binding energy by about 15%.

Calculations are performed by a plane-wave code and an efficient vdW algorithm[34] with Troullier-Martins type norm-conserving pseudopotentials. Spot comparison with all electron calculations using large basis sets indicates a calculational accuracy of $\sim$1%, actually better than that of most of PAW potentials supplied in various standard codes. Large box sizes were used to control spurious electrostatic interactions between replicas. See Supplemental Material for further details.

Figure 1 shows a typical PEC for each kind of interaction. To make a direct comparison to the QC results, the PECs are calculated at the same geometry of those of the CCSD(T) PEC calculations[24] (shown as dash-dotted lines with circles), where each molecule is kept in its S22 geometry[25] and moved along the line defined by the center-of-mass coordinates of two molecules with-

out any rotation. Overall, the vdW-DF2 PECs (solid lines) show a remarkable agreement with QC ones for all separations and for all three types of interactions. The shapes of the PECs near the minima, important for vibrational frequencies, are greatly improved (see inset figures where PECs are aligned to have the common minimum point). More importantly the strength of vdW attraction at larger distances is weakened in agreement with QC, especially for vdW-bonded duplexes (Fig. 1(b)). In other words, the original vdW-DF overestimates vdW attraction at intermediate separations beyond the equilibrium separation, although its minimum energy is accurate. This has special importance in sparse condensed matter. An example will be given below.

The PECs tend to turn up slightly earlier when approaching the repulsion regime at small separations. This quite universal feature might be due to PW86 exchange functional which is slightly more repulsive than HF at short distances.[19] For duplexes whose large distance asymptote is dominated by dispersion (here methane dimer, ethene dimer, and benzene–methane), vdW-DF2 will have weaker attraction in the asymptotic region and smaller C_6 coefficients than vdW-DF, which (at least for the methane dimer) already gives a C_6 coefficient close to experiment.[6] Recently, this prediction was verified in detail for various duplexes.[35] However, in the region of our calculations, such deterioration is not pervasive. In any case, neither the vdW-DF curves nor the QC curve have reached their asymptotic limit for any of the above three cases. The remainder of the 22 duplexes have asymptotic forms dominated by electrostatics.

In Fig. 2, we summarize the calculated binding energies at equilibrium separation, at equilibrium separation plus 1 Å, and the equilibrium separations themselves, with each quantity given as a deviation from that implied by the reference calculations.[24–26] Each subfigure clearly shows one of the three major improvements: *(i) Hydrogen-bond strengths.* The mean absolute deviation (MAD) of binding energy for hydrogen-bonded duplexes is decreased from 91 to 40 meV. *(ii) Interaction at intermediate separations.* The MAD of binding energy at a separation 1 Å larger than the equilibrium one is reduced from 35 to 8 meV for the dispersion dominated group and also substantially for the mixed group. *(iii) Equilibrium separations.* MAD is reduced from 0.23 to 0.13 Å. *Overall*, the vdW-DF2 binding energies are within 50 meV of the reference except for duplexes 5 and 7. The MAD of binding energy is decreased from 41 to 22 meV (13% to 7.6%). As a final tidbit, we note that in vdW-DF2 the MAD for the equilibrium energy of the dispersion dominated complexes has been reduced to 11 meV, which is equal to the MAD of the work of Jurecka et al.,[25] which until very recently[26] was considered the 'gold standard' for accuracy in quantum chemical calculations on this group.

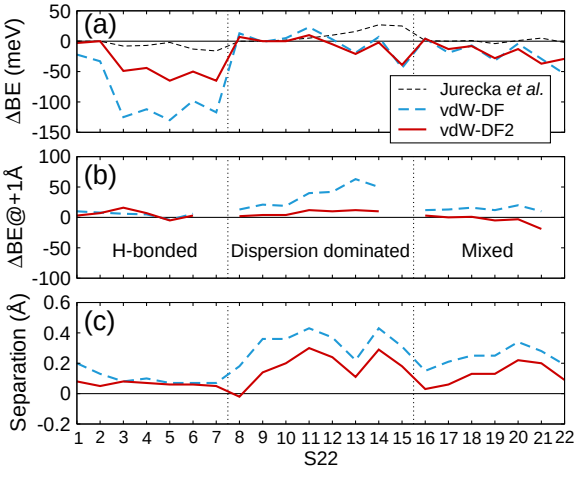

FIG. 2. (Color online) Comparison for the S22 duplexes of (a) binding energy predicted by Jurecka et al.,[25] vdW-DF,[4] and the present work (vdW-DF2). (b) binding energy at a separation 1 Å larger than the equilibrium one and, (c) equilibrium separations. The ordinates give the respective deviations of these quantities from the reference values taken from Takatani et al.[26] for panel (a), Molnar et al.[24] for panel (b), and Jurecka et al.[25] for panel (c).

The higher accuracy of vdW-DF2 persists in the extended systems we tested. As such applications, we calculated: (i) The graphite interlayer binding energy and spacing. The binding energy is on a par with that of vdW-DF which is already good. Interlayer spacing is about 2% shorter than that by vdW-DF, in better agreement with experiment. (ii) H_2 adsorption within two different metal-organic frameworks (MOFs), $Zn_2(BDC)_2(TED)$ and MOF-74. In the former, the binding at the highest binding site (57 meV including zero point) is in good agreement with heat of adsorption measurement (52 meV), whereas vdW-DF overestimates it by 60%. This demonstrates the importance of accurate intermediate-range interaction. For comparison, the binding energy of hydrogen to benzene, one of building blocks of $Zn_2(BDC)_2(TED)$, is almost the same for both functionals at the equilibrium separation. At larger separations, however, vdW-DF substantially overestimates the binding. In case of MOF-74, H_2 positions are experimentally known. VdW-DF2 shows its higher accuracy in predicting separations between hydrogens and nearby atoms (improved by 0.1-0.2 Å). The strongest binding comes from an unsaturated metal atom, rather than more distant structures, and the binding energy, already accurate in vdW-DF, is little changed in vdW-DF2. We also tested vdW-DF2 on the internal structure of a water molecule, as an example of strong chemical bonds in molecules. We find that vdW-DF2 is on par with PBE. For details of all tests, see Supplemental Material.

In summary, we have presented an enhanced version of vdW-DF, denoted by vdW-DF2, which can be implemented via simple modifications of existing codes. It results in significant improvements in equilibrium spacings between noncovalently bound complexes, as well as in binding energy, especially when hydrogen bonding plays

a role. We make a full comparison of PECs of both functionals with accurately known results for a set of 22 complexes and also apply it to extended solid systems, finding favorable results for the new functional. Thus, we expect our method to have important applications in a wide range of fields, including condensed matter and materials physics, chemical physics, and the physics of biological materials.

We thank V. Cooper, A. Gulans, and R. Nieminen for discussions, P. Elliott and K. Burke for an early copy of Ref. 17, and D. Case for the use of his computer cluster for several spot checks. Work principally supported by NSF-DMR-0801343; work on MOFs by DE-FG02-08ER46491; DCL work at KITP by NSF-PHY05-51164; BIL work by the Lundbeck Foundation via CAMD.

[1] Y. Andersson, D. C. Langreth, and B. I. Lundqvist, Phys. Rev. Lett. **76**, 102 (1996).
[2] J. F. Dobson and B. P. Dinte, Phys. Rev. Lett. **76**, 1780 (1996).
[3] W. Kohn, Y. Meir, and D. E. Makarov, Phys. Rev. Lett. **80**, 4153 (1998).
[4] M. Dion and others, Phys. Rev. Lett. **92**, 246401 (2004).
[5] T. Thonhauser and others, Phys. Rev. B **76**, 125112 (2007).
[6] A recent variant denoted vdW-DF-09 by its authors [O. A. Vydrov and T. Van Voorhis, J. Chem. Phys. **130**, 104105 (2009)] introduces some empiricism, but has been applied to too few systems to assess usefulness. A more recent functional [O. A. Vydrov and T. Van Voorhis, Phys. Rev. Lett. **103**, 063004 (2009)] has been the subject of further discussion [D. C. .Langreth and B. I. Lundqvist, Phys. Rev. Lett. **104**, 099303 (2010); O. A. Vydrov and T. Van Voorhis, Phys. Rev. Lett. **104**, 099304 (2010)].
[7] D. C. Langreth and others, J. Phys.: Condens. Matter **21**, 084203 (2009).
[8] A. Puzder, M. Dion, and D. C. Langreth, J. Chem. Phys. **124**, 164105 (2006).
[9] S. D. Chakarova-Käck, E. Schröder, B. I. Lundqvist, and D. C. Langreth, Phys. Rev. Lett. **96**, 146107 (2006).
[10] L. Kong, G. Román-Pérez, J. M. Soler, and D. C. Langreth, Phys. Rev. Lett. **103**, 096103 (2009).
[11] K. Toyoda and others, Surf. Sci. **603**, 2912 (2009).
[12] L. Romaner and others, New J. Phys. **11**, 053010 (2009).
[13] A. Gulans, M. J. Puska, and R. M. Nieminen, Phys. Rev. B **79**, 201105(R) (2009).
[14] A. K. Kelkkanen, B. I. Lundqvist, and J. K. Nørskov, J. Chem. Phys **131**, 046102 (2009).
[15] J. P. Perdew and Y. Wang, Phys. Rev. B **33**, 8800(R) (1986).
[16] We recommend the refitted version PW86R (see Ref. 19, Table 2) for increased accuracy on the ∼1% level. It was used for the vdW-DF2 calculations here.
[17] P. Elliott and K. Burke, Canadian J. Chem. **87**, 1485 (2009).
[18] Y. Zhang and W. Yang, Phys. Rev. Lett. **80**, 890 (1998).
[19] E. D. Murray, K. Lee, and D. C. Langreth, J. Chem. Theory Comput. **5**, 2754 (2009).
[20] V. R. Cooper, Phys. Rev. B **81**, 161104 (2010).
[21] J. Klimes, D. R. Bowler, and A. Michaelides, J. Phys.:Condens. Matter **22**, 022201 (2010).
[22] F. O. Kannemann and A. D. Becke, J. Chem. Theory Comput. **5**, 719 (2009).
[23] VdW-DF with PW86 exchange corrects equilibrium separations, but overestimates bindings and vdW attractions beyond equilibrium separations which will be fixed by new vdW-DF2 correlation kernel. See Fig.4 in Supplemental Material.
[24] L. F. Molnar, X. He, B. Wang, and J. Kenneth M. Merz, J. Chem. Phys. **131**, 065102 (2009).
[25] P. Jurecka, J. Sponer, J. Cerný, and P. Hobza, Phys. Chem. Chem. Phys. **8**, 1985 (2006).
[26] T. Takatani and others, J. Chem. Phys. **132**, 144104 (2010).
[27] D. C. Langreth and S. H. Vosko, Adv. Quantum Chem. **21**, 175 (1990).
[28] The second order expansion of the vdW interaction, the "c" term in the notation of Ref. 27, was omitted, so that only the "a" and "b" terms are retained, hence the notation Z_{ab}. See Appendix B of Ref. 5. for a full discussion.
[29] The relation between Z and other notations for the gradient coefficient: $Z = -9\mu = -48\pi(3\pi^2)^{1/3}\beta$. For pure exchange, $Z = -10/9$ in the gradient expansion, while for B88, $Z = -2.469$.
[30] J. Schwinger, Phys. Rev. A **22**, 1827 (1980).
[31] J. Schwinger, Phys. Rev. A **24**, 2353 (1981).
[32] A. D. Becke, Phys. Rev. A **38**, 3098 (1988).
[33] This screening term is considerably smaller than the gradient exchange term. We expect that as an estimate, we can without major overall error simply assume that it increases in the same proportion as gradient exchange itself. This ansatz, unlike other simple approaches we might have taken, also assures that the effect of the 10/7 factor enhancing Sham exchange continues to cancel out of exchange and correlation together as it should.[27]
[34] G. Román-Pérez and J. M. Soler, Phys. Rev. Lett. **103**, 096102 (2009). We adapted SIESTA [P. Ordejón, E. Artacho and J. M. Soler, Phys. Rev. **53**, 10441(R) (1996); J. M. Soler *et al.*, J. Phys.: Condens. Matt. **14**, 2745 (2002)] vdW code for use within a modified version of ABINIT [X. Gonze *et al.*, Comp. Mat. Sci. **25**, 478 (2002)]. The vdW interaction was treated fully self-consistently including forces. The computational costs are the same with vdW-DF. See Supplemental Material for more details.
[35] O. Vydrov and T. Van Voorhis, Phys. Rev. A **81**, 062708 (2010).

Supplemental Material

Computational details The convergence control parameters for the plane-wave pseudopotential calculations are tuned until the binding energy is converged up to 0.4 meV (0.01 kcal mol^{-1}). We used 50 Rydberg kinetic-energy cutoff for hydrocarbon systems and 60 Rydberg for all the others containing nitrogen and oxygen. For polar molecules with large dipole moments a 60×60×60 Bohr^3 cubic unit cell is needed to eliminate spurious elec-

trostatic interaction between supercell images. The accuracy of the pseudopotentials are tested within PBE [J. Perdew, K. Burke, and M. Ernzerhof, Phys. Rev. Lett. **77**, 3865 (1996)] by comparing with all-electron results for the water dimer (duplex #2 in S22) and formic acid dimer (duplex #3). The all-electron energies obtained were also converged to the level of 0.4 meV (See Table I). For water dimer we obtained binding energies (in meV) of 215 (all electron) and 219 (pseudopotential). Similarly, for the formic acid dimer we obtained 790 (all electron) and 798 (pseudopotential). The respective deviations are thus 2% and 1%.

Compared to GGA, the vdW-DF2 computation time per iteration roughly doubled for the smaller S22 duplex calculations, but the increase becomes virtually unmeasurable for the larger MOF systems that have more than 100 atoms per unit cell. The number of iterations required for convergence is also typically comparable to that of GGA, but in some MOF cases it is almost doubled.

TABLE I. Convergence of all-electron PBE binding energy (in meV) of the water dimer (duplex #2 in S22) and the formic acid dimer (duplex #3). The calculations are performed by Gaussian03.[a] Dunning's correlation consistent basis sets with diffuse functions are used, with counterpoise-corrections.

basis set	water dimer	formic acid dimer
aug-cc-pVDZ	212	774
aug-cc-pVTZ	213	784
aug-cc-pVQZ	214	790
aug-cc-pV5Z	215	790
aug-cc-pV6Z	215	–

[a] Gaussian 03, Revision E.01, M. J. Frisch, G. W. Trucks, H. B. Schlegel, G. E. Scuseria, M. A. Robb, J. R. Cheeseman, J. A. Montgomery, Jr., T. Vreven, K. N. Kudin, J. C. Burant, J. M. Millam, S. S. Iyengar, J. Tomasi, V. Barone, B. Mennucci, M. Cossi, G. Scalmani, N. Rega, G. A. Petersson, H. Nakatsuji, M. Hada, M. Ehara, K. Toyota, R. Fukuda, J. Hasegawa, M. Ishida, T. Nakajima, Y. Honda, O. Kitao, H. Nakai, M. Klene, X. Li, J. E. Knox, H. P. Hratchian, J. B. Cross, V. Bakken, C. Adamo, J. Jaramillo, R. Gomperts, R. E. Stratmann, O. Yazyev, A. J. Austin, R. Cammi, C. Pomelli, J. W. Ochterski, P. Y. Ayala, K. Morokuma, G. A. Voth, P. Salvador, J. J. Dannenberg, V. G. Zakrzewski, S. Dapprich, A. D. Daniels, M. C. Strain, O. Farkas, D. K. Malick, A. D. Rabuck, K. Raghavachari, J. B. Foresman, J. V. Ortiz, Q. Cui, A. G. Baboul, S. Clifford, J. Cioslowski, B. B. Stefanov, G. Liu, A. Liashenko, P. Piskorz, I. Komaromi, R. L. Martin, D. J. Fox, T. Keith, M. A. Al-Laham, C. Y. Peng, A. Nanayakkara, M. Challacombe, P. M. W. Gill, B. Johnson, W. Chen, M. W. Wong, C. Gonzalez, and J. A. Pople, Gaussian, Inc., Wallingford CT, 2004.

TABLE II. Internal structure of a free water molecule. The bond length and bond angle calculated by vdW-DF2, vdW-DF, and PBE well agree each other within 0.002 Å and 0.7 degree. Norm-conserving pseudopotentials (NCPP), 20×20×20 Bohr^3 cubic unit cell, 130 Rydberg kinetic-energy cutoff, and 0.002 eV/Å force tolerance are used. For comparison all-electron (AE) PBE, CCSD(T), and experiment values are given as well. AE PBE bond length is 0.007–0.009 Å longer than our pseudopotential calculation.

Method	d(OH) (Å)	θ(HOH) (°)
vdW-DF2 (NCPP)	0.960	105.0
vdW-DF (NCPP)	0.960	104.7
PBE (NCPP)	0.962	104.3
PBE (AE)	0.969[a], 0.971[b]	104.1[b]
CCSD(T)[c]	0.958	104.5
Expt.[d]	0.958	104.5

[a] All-electron calculation with the def2-TZVPP basis set (triple-ζ quality including high exponent polarization functions), which is a larger basis set than the cc-pCVTZ basis set, taken from J. Chem. Phys. **126**, 124115 (2007).

[b] All-electron calculation with aug-cc-pVTZ basis set taken from J. Phys. Chem. A **108**, 2305 (2004).

[c] D. Feller and K. A. Peterson, J. Chem. Phys. **131**, 154306 (2009).

[d] S. V. Shirin *et al.*, J. Mol. Spectrosc. **236**, 216 (2006).

TABLE III. Comparison of binding energy and equilibrium separation. The latter is given as a deviation from the original S22 geometry[a] along the center-of-mass line, as shown in the first data column of Table IV).

#	Duplex	Binding energy (meV)				Separation (Å)	
		vdW-DF	vdW-DF2	QC[a]	QC[b]	vdW-DF	vdW-DF2
1	Ammonia dimer	115	134	137	137	0.20	0.08
2	Water dimer	185	218	218	218	0.13	0.05
3	Formic acid dimer	690	766	807	815	0.08	0.08
4	Formamide dimer	587	655	692	699	0.10	0.07
5	Uracil dimer	767	832	895	897	0.07	0.06
6	2-pyridoxine·2-aminopyridine	639	687	725	737	0.07	0.06
7	Adenine·thymine	609	660	710	726	0.07	0.05
8	Methane dimer	36	30	23	23	0.18	−0.02
9	Ethene dimer	64	65	65	65	0.36	0.14
10	Benzene·methane	68	63	65	63	0.36	0.20
11	Benzene dimer (slip-parallel)	136	123	118	114	0.43	0.30
12	Pyrazine dimer	185	177	192	182	0.36	0.24
13	Uracil dimer (stacked)	403	402	439	422	0.22	0.11
14	Indole·benzene (stacked)	206	197	226	199	0.42	0.29
15	Adenine·thymine (stacked)	461	466	530	506	0.30	0.18
16	Ethene·ethine	69	70	66	65	0.15	0.03
17	Benzene·water	124	129	142	143	0.20	0.06
18	Benzene·ammonia	94	92	102	101	0.27	0.13
19	Benzene·HCN	166	170	193	197	0.24	0.13
20	Benzene dimer (T-shape)	113	105	119	118	0.34	0.22
21	Indole·benzene (T-shape)	214	206	248	243	0.28	0.20
22	Phenol dimer	254	279	306	307	0.19	0.09
	Mean deviation (MD)	−36	−21	2		0.23	0.13
	Mean absolute deviation (MAD)	41	22	7		0.23	0.13
	MAD%	13%	8%	2%			

[a] P. Jurecka, J. Sponer, J. Cerný, and P. Hobza, Phys. Chem. Chem. Phys. **8**, 1985 (2006).
[b] T. Takatani, E. G. Hohenstein, M. Malagoli, M. S. Marshall, and C. D. Sherrill, J. Chem. Phys. **132**, 144104 (2010).

TABLE IV. Left two data columns: The center-of-mass separations and the nearest neighbor (NN) pair separations in the S22 geometry of Jurecka *et al.* These center-of-mass distances corresponds to the zeros of the abscissa in the PEC plots in Figs. 1–4. The species of NN atom pair are given in the parentheses. Right two data columns: The deviations from the CCSD(T) value [J. Chem. Phys. **131**, 065102 (2009)] of the binding energy at a distance 1 Å larger than that of the S22 equilibrium geometry of Jurecka *et al.* [Phys. Chem. Chem. Phys. **8**, 1985 (2006)].

#	Duplex	Separation (Å)		ΔBE at +1 Å (meV)	
		Center-of-mass	NN pair	vdW-DF	vdW-DF2
1	Ammonia dimer	3.21	2.50 (NH)	10	3
2	Water dimer	2.91	1.95 (OH)	8	7
3	Formic acid dimer	2.99	1.67 (OH)	6	16
4	Formamide dimer	3.23	1.84 (OH)	5	7
5	Uracil dimer	6.07	1.77 (OH)	−4	−5
6	2-pyridoxine·2-aminopyridine	5.14	1.86 (NH)	6	3
7	Adenine·thymine	5.97	1.82 (NH)	N/A[a]	N/A[a]
8	Methane dimer	3.72	3.51 (CH)	13	2
9	Ethene dimer	3.72	2.56 (HH)	21	4
10	Benzene·methane	3.72	2.79 (CH)	19	4
11	Benzene dimer (slip-parallel)	3.76	3.37 (CC)	40	12
12	Pyrazine dimer	3.48	3.27 (NH)	42	10
13	Uracil dimer (stacked)	3.17	2.71 (OH)	63	12
14	Indole·benzene (stacked)	3.50	3.20 (CH)	50	10
15	Adenine·thymine (stacked)	3.17	2.68 (HH)	N/A[a]	N/A[a]
16	Ethene·ethine	4.42	2.83 (CH)	12	3
17	Benzene·water	3.38	2.60 (CH)	13	0
18	Benzene·ammonia	3.56	2.77 (CH)	16	1
19	Benzene·HCN	3.95	2.67 (CH)	12	−5
20	Benzene dimer (T-shape)	4.91	2.80 (CH)	20	−3
21	Indole·benzene (T-shape)	4.88	2.59 (CH)	10	−19
22	Phenol dimer	4.92	1.94 (OH)	N/A[a]	N/A[a]
	Mean deviation (MD)			19	3
	Mean absolute deviation (MAD)			19	7
	MAD%			16%	4%

[a] The CCSD(T) PEC is not available.

TABLE V. Graphite interlayer binding energy and interlayer spacing (i.e., half of the c lattice constant). An AB stacked 4-layer unit cell is used for vdW-DF and vdW-DF2 calculations. The interlayer binding energy is calculated by subtracting the energy of each single layer in the same unit cell from that of 4-layer infinite bulk.

	vdW-DF	vdW-DF2	QMC[a]	Experiment[b]
Binding energy (meV/atom)	50	49	56±5	52±5
Interlayer spacing (Å)	3.60	3.53	3.43	3.36

[a] L. Spanu, S. Sorella, and G. Galli, Phys. Rev. Lett. **103**, 196401 (2009). Zero-point energy and phonon contributions at 300K are included.

[b] R. Zacharia, H. Ulbricht, and T. Hertel, Phys. Rev. B **69**, 155406 (2004).

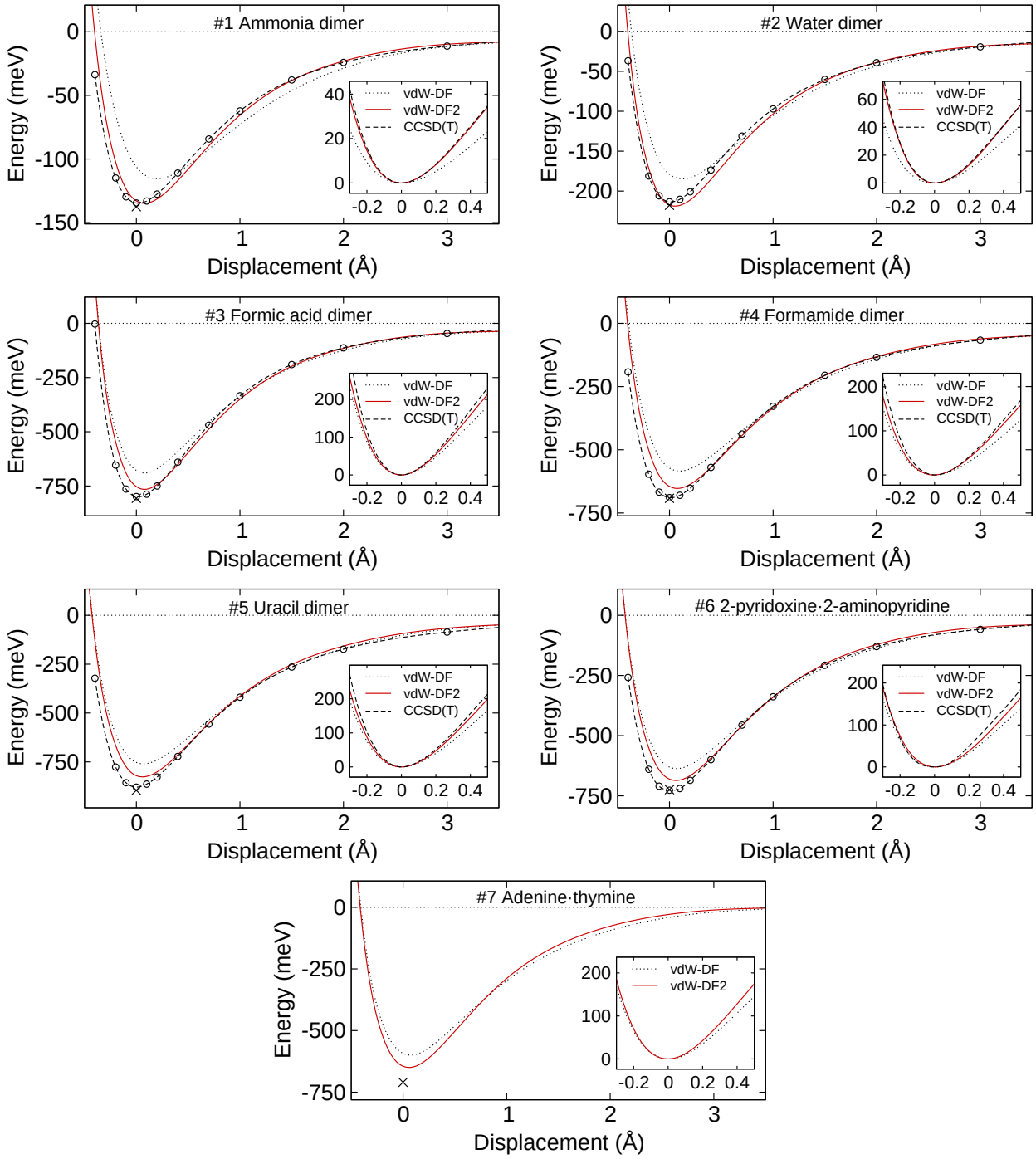

FIG. 1. Potential energy curves (PECs) of hydrogen-bonded duplexes. The S22 data points (cross marks) are taken from T. Takatani, E. G. Hohenstein, M. Malagoli, M. S. Marshall, and C. D. Sherrill, J. Chem. Phys. **132**, 144104 (2010). The CCSD(T) PECs data (dashed lines with open circles) in this and subsequent figures are taken from L. F. Molnar, X. He, B. Wang, and J. Kenneth M. Merz, J. Chem. Phys. **131**, 065102 (2009). For the hydrogen-bonded adenine-thymine duplex, CCSD(T) PEC data is not available. The shapes near minima are compared in inset figures where PECs are aligned to have the common minimum point.

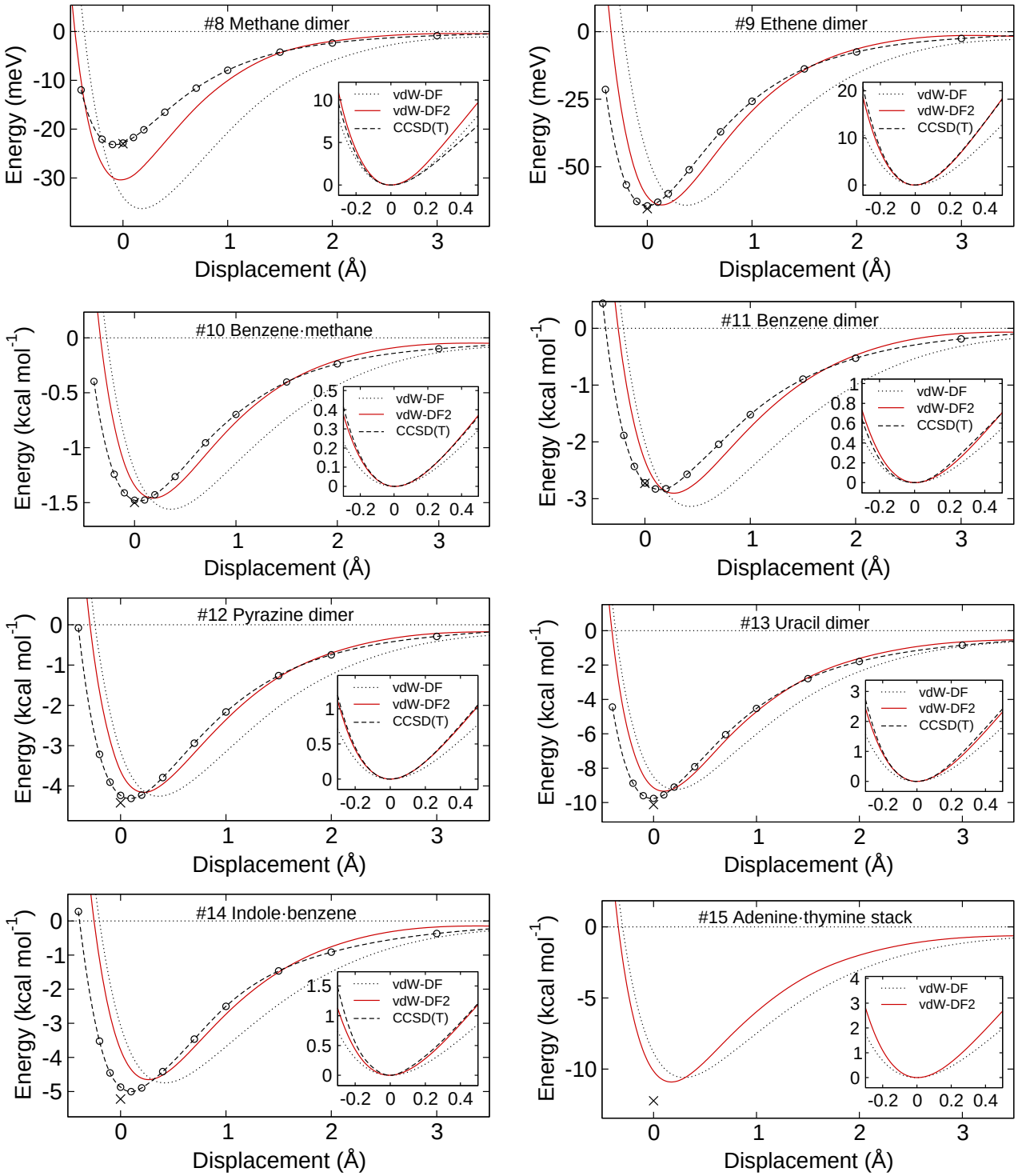

FIG. 2. Potential energy curves (PECs) of dispersion-dominated duplexes. For the stacked adenine-thymine duplex, CCSD(T) PEC is not available. The S22 data points (cross marks) are taken from T. Takatani, E. G. Hohenstein, M. Malagoli, M. S. Marshall, and C. D. Sherrill, J. Chem. Phys. **132**, 144104 (2010). The original S22 values (plus marks taken from P. Jurecka, J. Sponer, J. Cerný, and P. Hobza, Phys. Chem. Chem. Phys. **8**, 1985 (2006)) are also shown if the difference between those two values are larger than 3%.

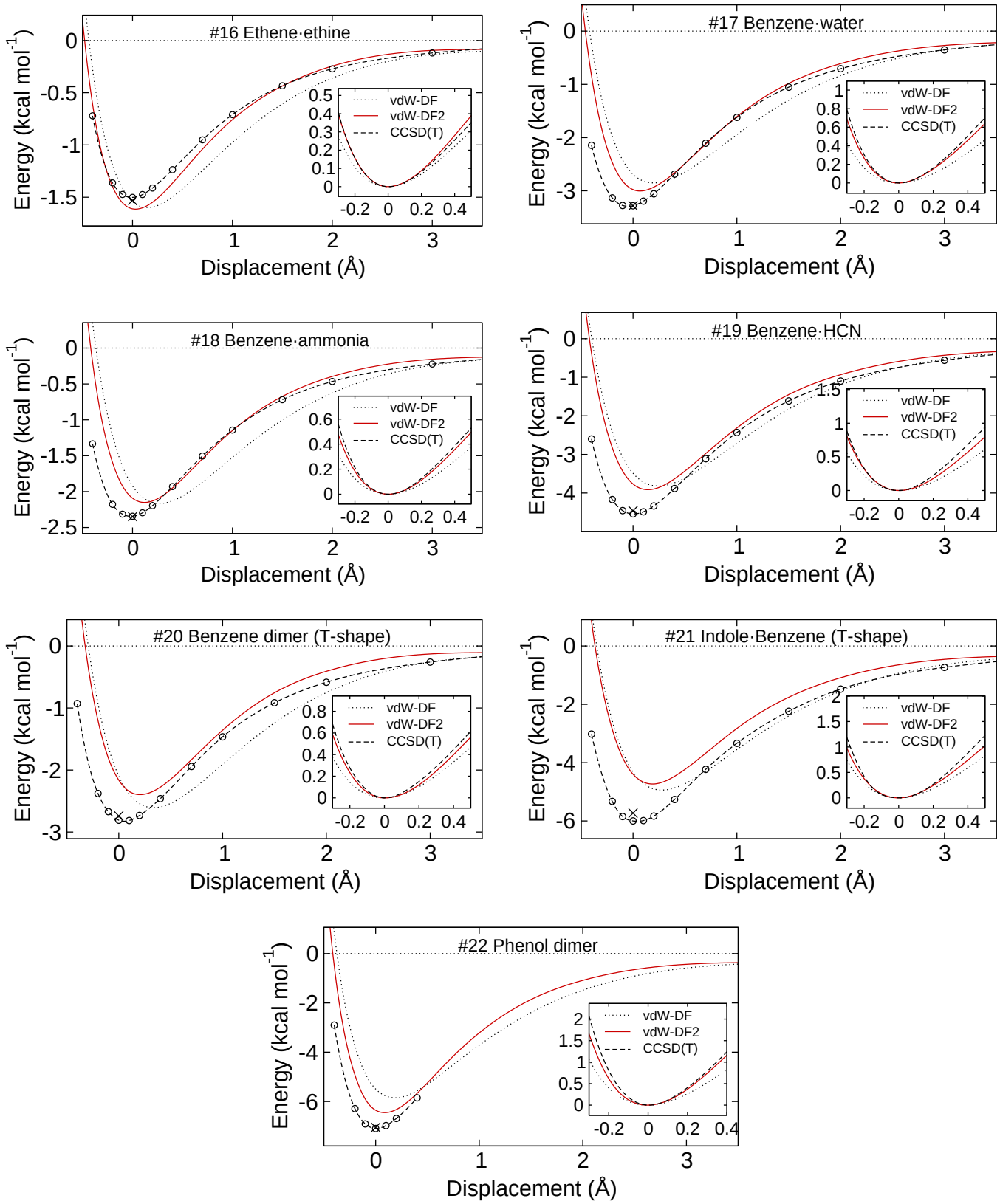

FIG. 3. Potential energy curves (PECs) of mixed interaction duplexes.

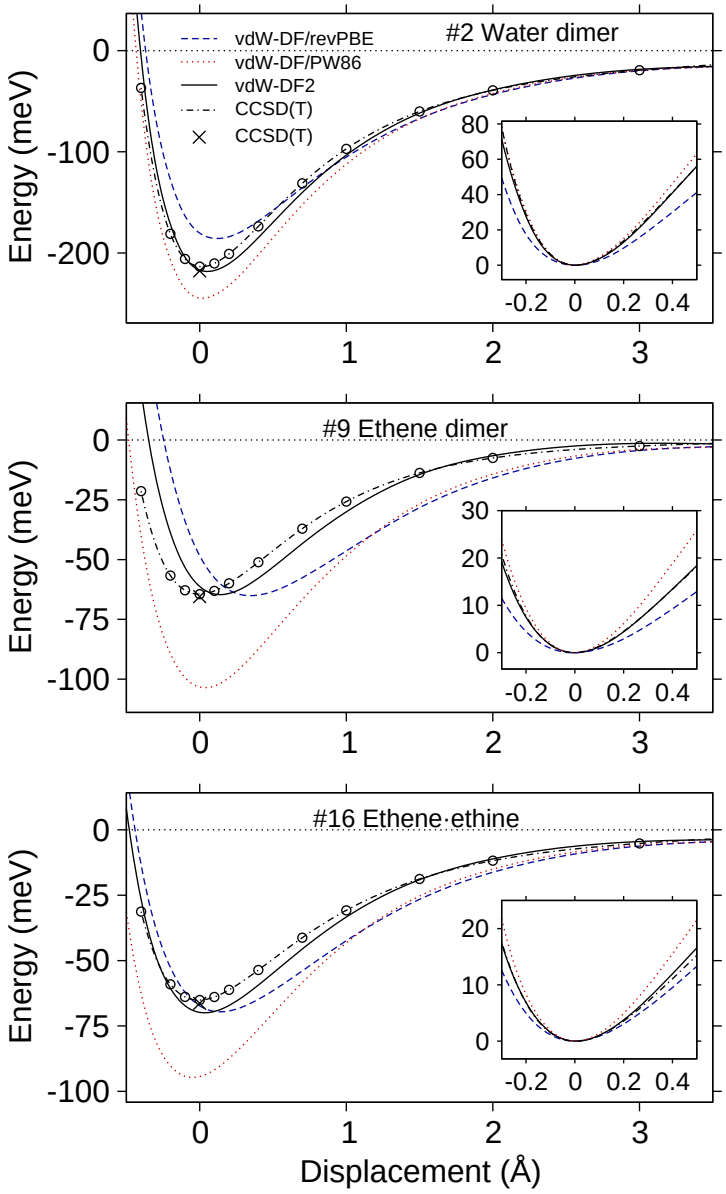

FIG. 4. Comparison of vdW-DF with revPBE exchange functional (vdW-DF/revPBE), vdW-DF with PW86R (vdW-DF/PW86R), and vdW-DF2 with PW86R (vdW-DF2). Potential energy curves (PECs) of water dimer (hydrogen-bonded duplexes), ethene dimer (dispersion), ethene-ethine duplex (mixed) are shown. Note that the difference between vdW-DF/revPBE and vdW-DF/PW86R vanishes beyond 1 Å. Replacing revPBE exchange with PW86 weakens the repulsion near equilibrium separations and gives more accurate separations but also large overbinding. Furthermore, the comparison of PECs with CCSD(T) shows that the original vdW-DF consistently overestimates the vdW attraction. The use of large-N asymptote in determining the internal functional for vdW kernel effectively weakens the vdW attraction and vdW-DF2 gives an excellent agreement with CCSD(T) for all separations.

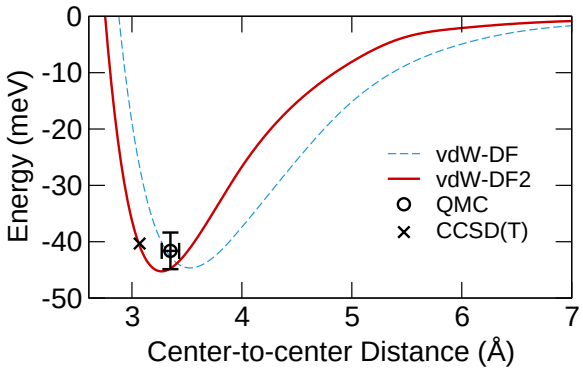

FIG. 5. Hydrogen-benzene potential energy curve (PEC). Sampled along a normal vector of the benzene plane passing through the benzene center. H_2 is parallel to the vector. The CCSD(T) result is taken from Hübner *et al.* J. Phys. Chem. A **108**, 3019 (2004) and QMC from Beaudet *et al.* J. Chem. Phys. **129**, 164711 (2008).

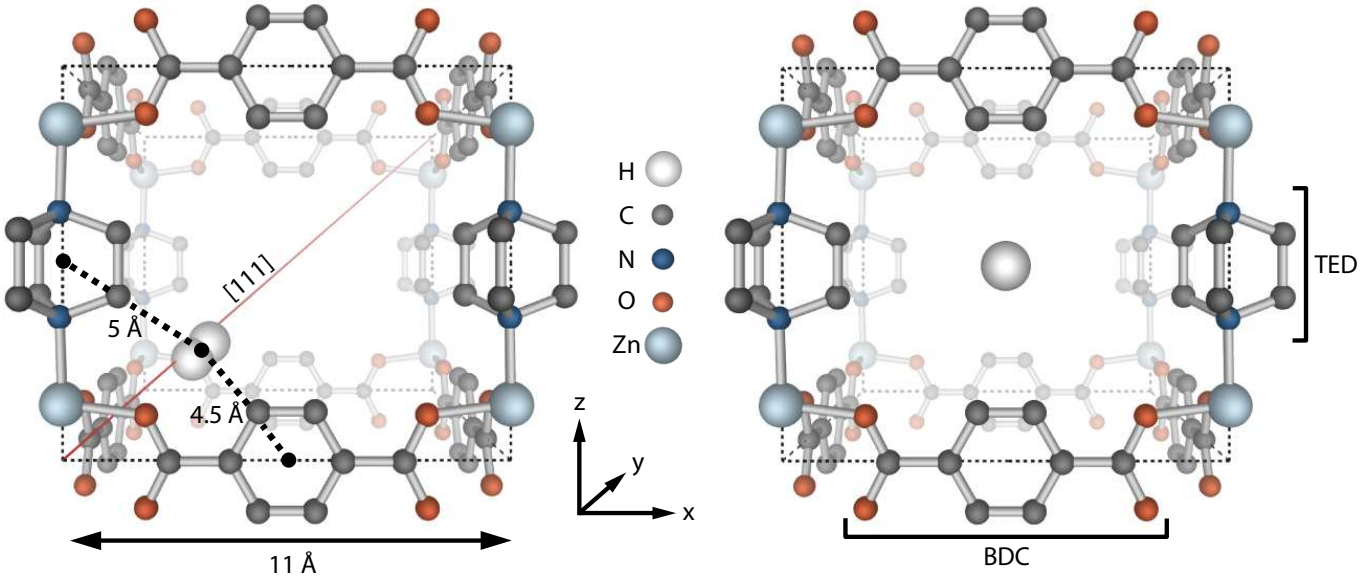

FIG. 6. Hydrogen adsorption by the metal-organic framework (MOF) structure $Zn_2(BDC)_2(TED)$ where BDC and TED denote the linking structures so labeled above. Hydrogen atoms attached to carbon atoms are removed for simplicity. The left panel shows the H_2 in a "corner" site along the body diagonal, and the right panel shows the H_2 head-on in the "face center" site. The binding of the H_2 is dominated in both cases by its interactions with the benzene and TED complexes which are ∼5 Å away.

TABLE VI. Hydrogen binding energies in $Zn_2(BDC)_2(TED)$ (in meV). Zero-point energies are included in the calculated values. These values demonstrate the importance for the functional to give accurate interaction energies at intermediate distances that are longer than the equilibrium distances in isolated duplexes. For example, the hydrogen-benzene interaction (Fig. 5) at a center-to-center distance of 5 Å is ∼100% overestimated by vdW-DF, although the binding energy at the equilibrium separation is quite accurate. This effect leads to the 60% overestimate of the binding of the most strongly bound H_2 in the $Zn_2(BDC)_2(TED)$ crystal by vdW-DF. In vdW-DF2 the error reduced to a reasonable size, and a switching of which site is the most strongly bound also occurs.

H_2 binding site	H_2 binding energy (meV)		
	vdW-DF[a]	vdW-DF2	Expt.[b]
Corner site	74	65	52
Face-center site	82	56	

[a] L. Kong, V. R. Cooper, N. Nijem, K. Li, J. Li, Y. J. Chabal, and D. C. Langreth, Phys. Rev. B **79**, 081407(R) (2009).

[b] J. Y. Lee, D. H. Olson, L. Pan, T. J. Emge, and J. Li, Adv. Funct. Mater. **17**, 1255 (2007).

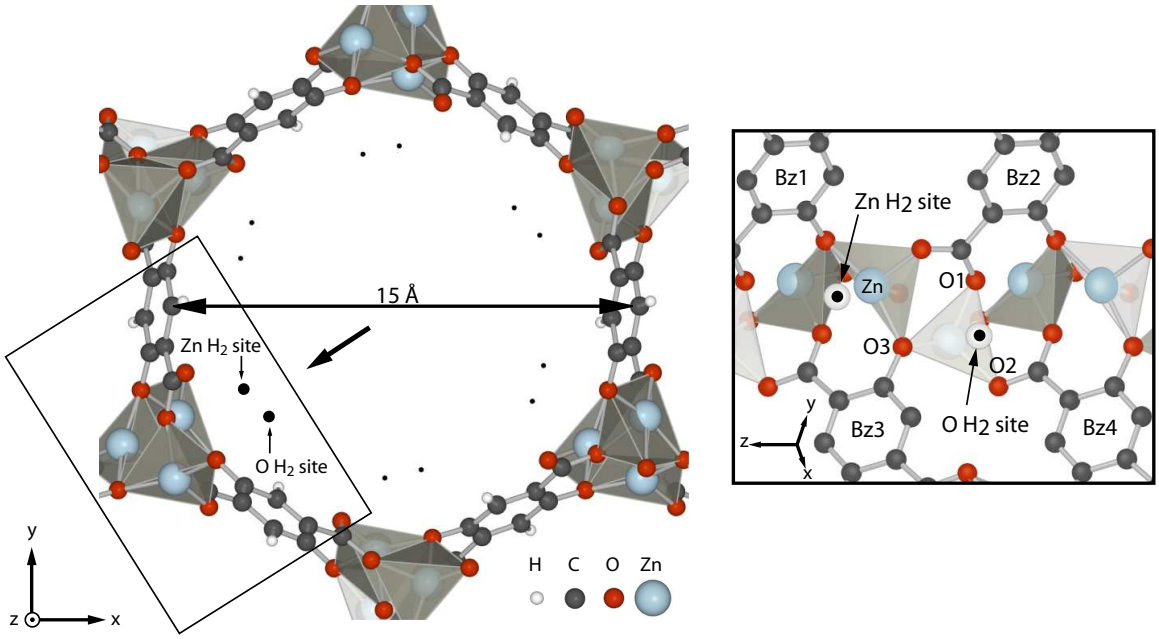

FIG. 7. Hydrogen adsorption sites (black dots) in MOF-74 [N. L. Rosi, J. Kim, M. Eddaoudi, B. Chen, M. O'Keeffe, and O. M. Yaghi, J. Am. Chem. Soc. **127**, 1504 (2005)]. (Left) Top view into the pore. (Right) Side view of the pore wall. The viewing direction and area are depicted by a short arrow and a rectangle, respectively, in the left figure.

TABLE VII. Equilibrium separations (in Å) of hydrogens to the nearest atom, to the nearest hydrogen, and to nearby benzene (Bz) rings in MOF-74. Calculated binding energies (including zero-point energies) of H_2 at Zn site are given at the last line. In this MOF, the binding is dominated by the proximity of the H_2 to the unsaturated Zn atom, and the accurate binding energy predicted by vdW-DF is essentially unchanged in vdW-DF2. Still, the weakening of the intermediate range attraction is presumably compensated by the closer proximity of the H_2 to the Zn atom in vdW-DF2.

From	To[c]	Distance (Å)		
		vdW-DF[a]	vdW-DF2	Expt.[b]
Zn H_2 site	Zn	3.0	2.8	2.6
	Bz1[d]	4.2	4.1	3.9
	Bz3[d]	4.4	4.3	4.2
	O H_2 site	3.3	3.1	2.9
O H_2 site	O1	3.7	3.4	3.3
	O2	4.3	4.0	3.5
	O3	3.4	3.3	3.1
	Bz2[d]	5.1	4.8	5.0
	Bz3[d]	4.7	4.7	4.6
	Bz4[d]	5.4	5.3	4.7
H_2 binding energy at Zn site (eV)		0.10	0.10	0.09

[a] L. Kong, G. Román-Pérez, J. M. Soler, and D. C. Langreth, Phys. Rev. Lett. **103**, 096103 (2009).
[b] Y. Liu, H. Kabbour, C. M. Brown, D. A. Neumann, and C. C. Ahn, Langmuir **24**, 4772 (2008).
[c] See the right panel of Fig. 7 for a depiction of the corresponding atomic locations.
[d] To the center of the molecule.

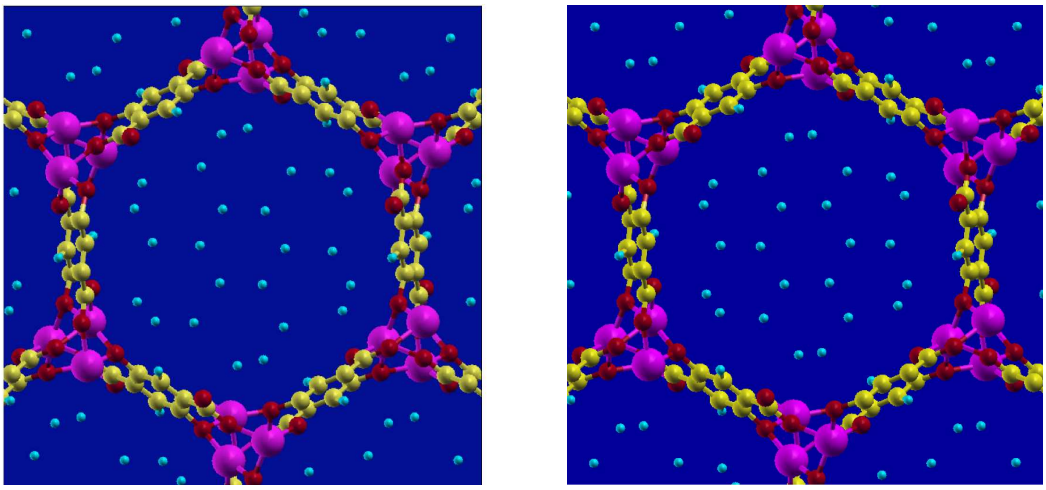

FIG. 8. D_2 adsorption sites in the fully loaded MOF-74: Via neutron diffraction[a] (left panel); Via vdW-DF2 (right panel).
[a]Y. Liu, H. Kabbour, C. M. Brown, D. A. Neumann, and C. C. Ahn, Langmuir **24**, 4772 (2008).